BeBeC-2020-D01

Sound field extrapolation with microphone arrays

Volker Becker, Christof Puhle, Alexander Jahnke and Dirk Döbler
GFaI e.V.
Volmerstraße 3, 12489, Berlin, Germany

Abstract

The use of microphone arrays for locating sound sources and determining their source levels using beamforming or near-field holography has been state of the art for many years. Typically, the object under investigation is located in front of a microphone array and the measured sound field is used to determine the sound levels on the object. For some applications, however, the development and propagation of the sound field behind the array is also of interest. Recently C. Puhle introduced a paper [9] about theoretical principles and methods in the form of the algorithm Spherical Integration Farfield Acoustic Holography (SIFAH) to address that issue. In the present work, we show first measurements with a microphone array optimized for both, beamforming and SIFAH. Sound sources at different positions in front of the array were measured, the sound field behind the array was extrapolated and compared with measurements of real microphones placed at different positions. The influence and the treatment of ground reflections in a semi-anechoic room are discussed and the achieved accuracy is represented by level profiles. Furthermore we show how the algorithm can be used to simulate the noise of a passing vehicle.

1 INTRODUCTION

Acoustic holography is of increasing relevance since the last decades. Established methods are e.g. the HELS method which is based on a decomposition into spherical harmonics [13] or the Nearfield Acoustical Holography which is often used to detect surface vibrations [3]. Recently Puhle [9, 10] presented a novel acoustic holography method based on spherical integration. This method is used here to extrapolate the sound field produced by different vehicles from close range measurements. A possible application is the simulation of the noise emissions off a pass-by in a test rig. Such simulation systems already exist, e. g. the PAK System of Müller BBM [11], which was used as reference system in the current work. The microphones of that system must be placed at the distance from the vehicle, from where the pass-by would be observed in real measurements in the open air (typically 7.5m). With the method presented here the

measurement microphones can be placed very close to the vehicle. This enables the possibility of pass-by simulations in smaller test rigs. However one needs much more microphones for this method.

The paper is organized as follows: In section 2 we give a very short introduction to the basic idea of the SIFAH algorithm. In section 3 we will describe, how we calculate sound levels from the SIFAH results. Finally in section 4 we present the measurement setup, we describe the calibration process and we show results of the SIFAH extrapolation in comparison with reference measurements both on fixed positions as well as for pass-by situations.

2 Spherical integration far field acoustic holography

In this section we give a short introduction of the basic idea of spherical integration far field acoustic holography (SIFAH)[9]. We assume that all sources of noise are comprised in a sphere of radius R_0 and that free field sound propagation outside the sphere applies. In the frequency domain, sound propagation is then described by the Helmholtz equation (see. e.g. [4, p. 321])

$$\Delta p(\mathbf{r},k) + k^2 p(\mathbf{r},k) = 0, \tag{1}$$

where $p \in \mathbb{R}$ is the sound pressure, k is the wave number, Δ stands for the Laplacian and $\mathbf{r} \in \mathbb{R}^3$ denotes the location. If the boundary condition of the pressure field on the sphere's surface: $r = |\mathbf{r}| = R_0$, is known: $p(|\mathbf{r}| = R, k) = f(\theta, \phi, k)$ and furthermore Sommerfeld's radiation condition [12] applies[1], the solution of (1) is completely determined. Thus the whole pressure field could be calculated in principle. In spherical coordinates, the solution of (1) can be represented as series of spherical harmonics (see [13])

$$p(r,\theta,\phi) = \sum_{l=0}^{\infty} \sum_{m=-l}^{l} A_{lm} \mathrm{H}_l^{(2)}(kr) \mathrm{Y}_l^m(\theta,\phi), \tag{2}$$

where Y_l^m is the spherical harmonic of degree l and order m, A_{lm} is the corresponding complex coefficient and H_l is the Hankel function of degree l. The coefficients A_{lm} can be calculated using the scalar product

$$A_{l,m}(k) = \mathrm{H}_l^{(2)}(kR_0) \int_\Omega \mathrm{d}\Omega \; f(\theta,\phi,k) \mathrm{Y}_l^{*m}(\theta,\phi), \tag{3}$$

where $\Omega \in \mathbb{R}^2$ is the sphere's surface. Once all coefficients are known, the sound field can be calculated at any position. However, in practice we can measure neither the whole sound field on the sphere's surface nor does the freefield condition apply. Puhle developed a method how to calculate a sufficiently good estimation of (3) using a finite number of microphones which are not necessarily located on the surface of the sphere [9, 10]. In section 3.1 we will consider ground reflections in order to overcome the limitations due to the assumption of free field sound propagation. The work of Puhle forms the basis for the present manuscript. In the following chapters the SIFAH algorithm is essentially treated as a black box, implementation details are only mentioned if it cannot be avoided.

[1] This is the case when no sound comes from infinity

3 Evaluation of the SIFAH data

As it is sketched in figure 1, a microphone array samples the sound field at all microphone positions. The SIFAH-extrapolation will be done separately for the left and the right hand side of the sound source.

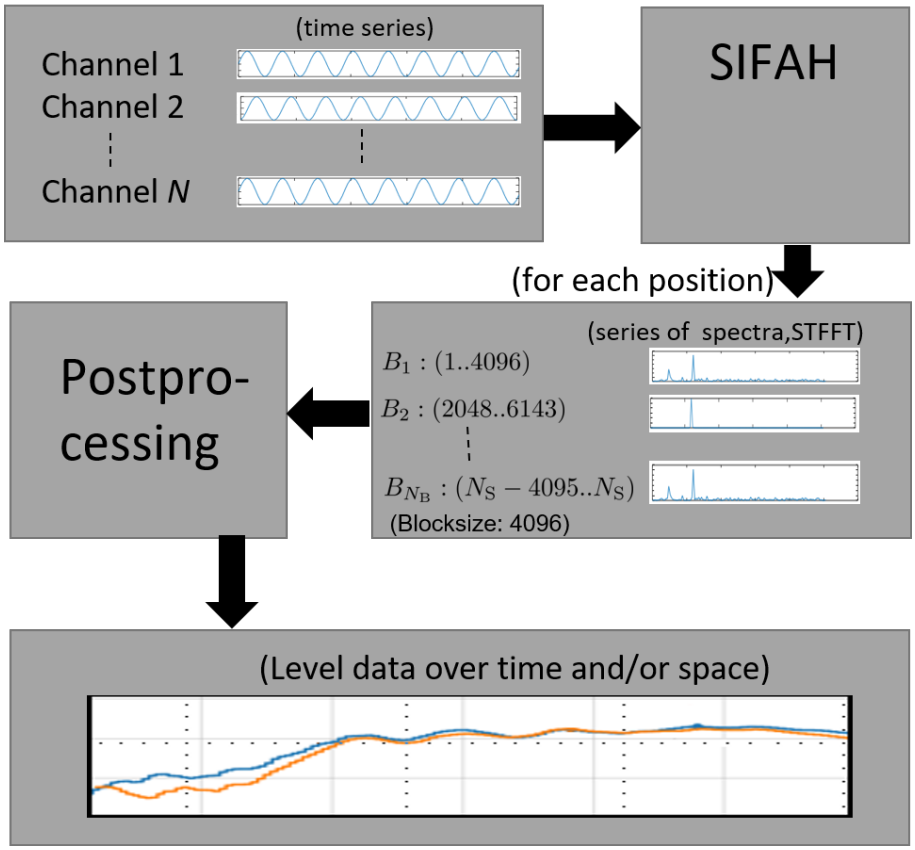

Figure 1: Sketch of the used calculation scheme: Time data measured on the microphone array, will be submitted to the SIFAH algorithm. The outcome is spectral data for short, overlapping time intervals. From this data we will generate level profiles as function of time, space, or both.

The time series recorded by the array, together with $M \in \mathbb{N}$ positions $\mathbf{r}_i, i \in \{i \leq M, i \in \mathbb{N}\}$ for which extrapolations should be produced (see [10]) will be submitted to the SIFAH module. The SIFAH module divides all measured time series in overlapping blocks of length $L \in \{2^n | n \in \mathbb{N}\}$ and performs a windowed FFT on the these blocks. Then the SIFAH algorithm, up to a maximal degree l_{max}, will be applied to every block. The outcome are M series of spectra which correspond to overlapping time intervals (blocks) of lengths L.

These M series of spectra are then treated as if they are the short time Fourier-transformations (STFFT) of the sound pressure at the corresponding positions. Remember that the application of an FFT to a finite time block assumes implicitly that the block is periodically continued. The SIFAH module estimates how a signal, represented in frequency domain, propagates in the space from the source within the reference sphere to another place outside the sphere. This

means, among other things, that the periodically repeated signal undergoes a phase shift due to the signal run-time between both places. With that fact in mind, it becomes clear that a transformation back into the time domain is not trivially possible. Even if the phase shifts were the only change to the data, transformed back to the time domain this would mean that a part of the curve slips from the end of a block to its beginning. If we try to reconnect such shifted time blocks to a resulting time series, it is obvious that the pressure curve becomes discontinuous and the result would sound strange. Nevertheless, the time evolution of the sound pressure levels can be estimated very well, as we will see later in this paper. One may analogously think of a signal splitted into short time intervals or blocks. The sound of an interval is played in a continuous loop and at some distance the sound level is measured and recorded in a protocol. This will be done for every block and the results can be composed to a curve of the entire signal.

A possible approach to receive a time signal nevertheless would be to consider only that samples which are not shifted over the edge of the block and choose a sufficiently large overlap so that the remaining samples from different blocks still overlap significantly. Finally one could apply a phase reconstruction algorithm like that of Griffin and Lim and its extension (e. g. [2, 5, 8]) to the STFFT. However, this is not in the scope of this paper.

For the following we define some denotations: With $\mathbf{B}_i(\mathbf{r}) \in \mathbb{C}^N$ we denote the i'th block of the SIFAH result on position $\mathbf{r}$. $B_{i,n}$ denotes the n'th sample of the i'th block. The time corresponding to the middle of the i'th block is referred as t_i. Let $S_i \in \mathbb{N}$ be the number of the sample which corresponds with the start sample of the i'th block in the time series. Furthermore let $f_s \in \mathbb{R}$ be the sampling rate, we find:

$$t_i = \frac{S_i + N/2}{f_s}. \tag{4}$$

We used the A-weighted RMS-Fast (see [7, chapter 2]) measure for evaluating effective values as required by ISO 362-1:2007 for pass-by measurements. Additionally we tested that other sound level measures work as well.

The A-weighted RMS-Fast is a measure with the intention of reproducing the human sense of hearing and is defined as:

$$p(t)^2_{(A)} = \frac{1}{\tau} \int_0^\infty \mathrm{d}t' \; p^2_{(A)}(t-t') e^{-\frac{t'}{\tau}}, \tag{5}$$

with $\tau = 125\text{ms}$, and $p_{(A)}$ is the A-filtered sound pressure. The corresponding sound level $L \in \mathbb{R}$ is defined as usual

$$L = 20 \cdot \log_{10} \frac{p(t)_{(A)}}{p_0}, \quad p_0 = 2 \cdot 10^{-5}\ \text{Pa}. \tag{6}$$

In the next section 3.1 we show how to extract level profiles for a fixed position in the room and in section 3.2 we will show a method to construct the curve which would be measured by a passing microphone.

3.1 Extrapolation of sound levels on fixed positions

Calculation of level data for free field propagation

Due to the fact that a reconstruction of the time series from the SIFAH result is not possible yet, we need a method to estimate the RMS-Fast directly from the STFFT data. According to the Parseval theorem we can estimate the A-weighted effective value at time t_i (see eq. (4)) within a frequency band corresponding to indices $k_{\min}, k_{\max}$ in the spectrum:

$$p_{\mathrm{A}}(t_i,\mathbf{r})^2 = \sum_{k_{\min}}^{k_{\max}} |A(k)B_{i,k}(\mathbf{r})|^2, \tag{7}$$

where $A(k) \in \mathbb{R}$ is the A-weight for the k'th coefficient. Using (7) as time series of the A-weighted sound pressure, (5) translates to:

$$p_{\mathrm{SIFAH}}(t)_A^2 = \frac{1}{N_{\mathrm{f}}} \sum_{i=1}^{Q(t)} \left(p_{\mathrm{A}}(t_i,\mathbf{r})^2\right) e^{-\frac{t-t_i}{\tau}},\ N_f = \sum_{i=1}^{Q(t)} e^{-\frac{t-t_i}{\tau}}. \tag{8}$$

The value of $Q(t) \in \mathbb{N}$ is the biggest possible number Q for which $t_Q <= t$ remains true.

This works well in free field as we have seen in simulations, however in real situations deviations between measured and extrapolated signals become significant. It turned out that we have to consider ground reflections.

The influence of ground reflections

Beside the SIFAH result on position $\mathbf{r}$ we also consider $B'_i = B(\mathbf{r}')$ where $\mathbf{r}'$ is the image of $\mathbf{r}$ mirrored on the ground. The n'th coefficient of the i'th resulting block $\mathbf{B}_i^{\mathrm{R}}$ is the sum of the spectrum of the directly arriving sound $\mathbf{B}_i$ and the spectrum of the reflected sound $\mathbf{B}'_i$ (see fig. 2):

$$B_{i,n}^{\mathrm{R}} = B'_{i,n} + \alpha(k)B_{i,n}. \tag{9}$$

Here $\alpha \in \{\mathbb{C} \mid |\alpha| \leq 1\}$ is a frequency dependent coefficient of reflection.

After a lot of test measurements and simulations (see also sec. 4) we found that the phase errors which occur in the SIFAH algorithm are to big to reproduce constructive and destructive interference between the reflected and the directly arriving sound correctly. We achieved better results[2] if we assumed that the reflected signal and the directly arriving signals are incoherent and interference terms vanish in mean. Under this assumption, the squared amplitude of the k'th coefficient in the resulting block can be written as

$$|B_{i,k}^{\mathrm{R}}|^2 = |B_{i,k}|^2 + |\alpha(k)|^2|B'_{i,k}|^2. \tag{10}$$

Based on the observation, that results become better if we choose $\alpha = 1$ for low frequencies and $\alpha = 0$ for high frequencies (ref. sec. 4), we used a simple model with two parameters to describe the reflections: The coefficient of reflection is identical to one in the frequencies range

[2] except for low frequency $f < 150$Hz

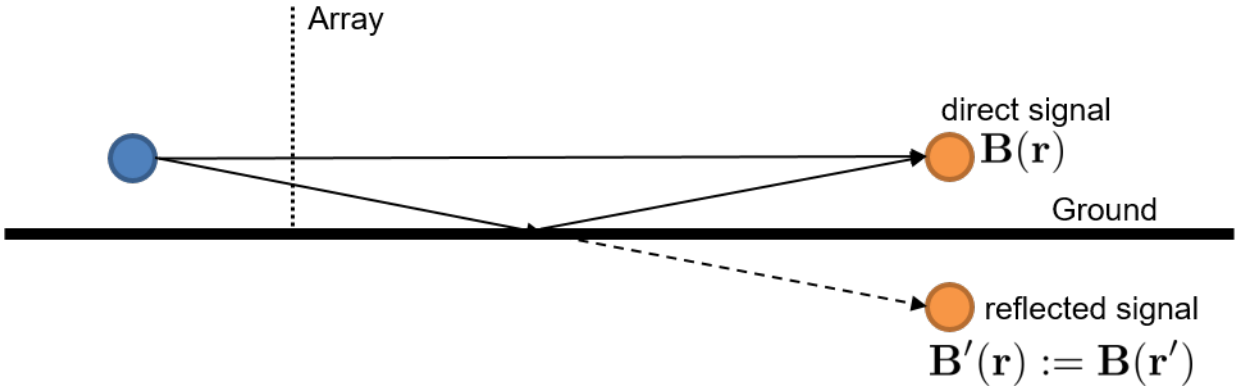

Figure 2: Sketch of the reflection treatment: The sound is extrapolated to the target position and also to its image mirrored on the ground. The two results are then added together.

$[0, f_l)$, in the range $[f_l, f_u)$ it decays linearly to zero and remains there for higher frequencies.

$$\alpha(f) = \begin{cases} 1.0 & \text{for} \quad f < f_l \\ 1 - \frac{(f-f_l)}{(f_u-f_l)} & \text{for} \quad f_l \leq f < f_u \\ 0.0 & \text{for} \quad f \geq f_u \end{cases} \tag{11}$$

This assumption is *qualitatively* similar to findings about reflections on rough surfaces and on reflections on acoustic black holes [6] in the literature.

Measure of deviation

To quantify the deviations of our extrapolations from the reference curves we define the following measure. Let $\mathbf{S} \in \mathbb{R}^N$ be the sampled SIFAH effective values, $R \in \mathbb{R}^N$ the sampled reference channel effective values, $D_i^2 = |S_i^2 - R_i^2|$ and $R_{\max} = \max(R_1, ..., R_N)$. Now the measure for the deviations between both signals is defined as:

$$\varepsilon_i := \varepsilon(R_{\max}^2, D_i^2) = 10 \cdot \log_{10}\left(\frac{R_{\max}^2 + D_i^2}{R_{\max}^2}\right) \geq 0. \tag{12}$$

This measure takes into account that the relative deviations near to the maximum of the curve are more relevant for practical applications than deviations elsewhere. Furthermore we define the maximal deviation

$$\varepsilon_{\max} = \varepsilon\left(R_{\max}^2, \max(D_i^2)\right) \tag{13}$$

and the mean deviation

$$\overline{\varepsilon} = \varepsilon\left(R_{\max}^2, \frac{1}{N}\sum_i D_i^2\right). \tag{14}$$

One can interpret that as if one takes the difference of a signal curve and a reference curve pretend that as if this would be the deviation on the reference curves maximum to calculate the

deviation in decibel.

3.2 Extrapolation of sound level for a moving observer

In this chapter we will show how to simulate a pass-by of a vehicle with SIFAH. In the real situation, the sound level at a position in a height of 1.2 meters and 7.5 meters from the middle of a road will be recorded while a vehicle starts pass-by at a distance of 15 meters and passes the observer. When it is 15 meters away in the other direction, the record is stopped. For the approval in the European Union a certain level shall not be exceeded during a pass-by at maximal acceleration, starting at velocity of 50 km/h.

To simulate a pass-by, using SIFAH, we calculate the A-weighted level curve of an imaginary microphone which moves in 7.5m distance and 1.2m height with the velocity $v_m(t) = -v_v(t)$ past the vehicle. Here $v_v(t)$ is the vehicles' velocity. Figure 3 gives a schematically illustration of the situation.

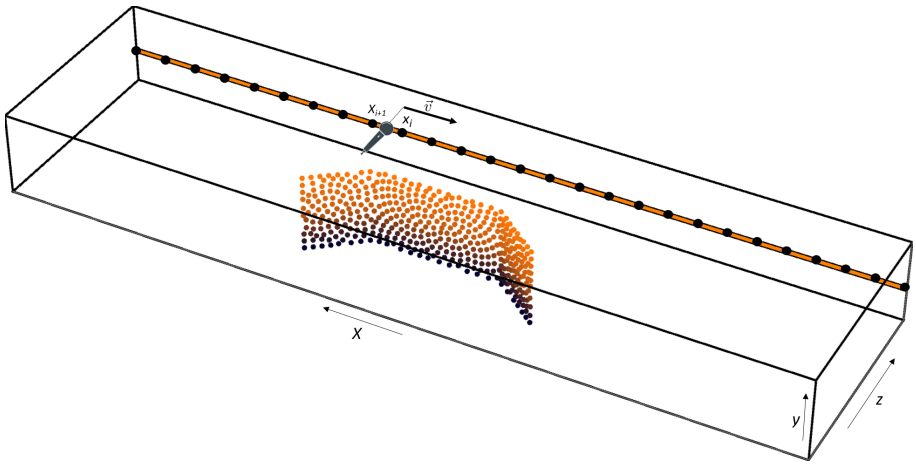

Figure 3: Representation of the SIFAH projection needed for the calculation of a pass-by. The sound field is measured with the microphones in the array, and extrapolated to positions x_i within the yellow stripe. Within this stripe an imaginary microphone is thought to move with the same speed as the vehicle would move on the road. From that the level curve of the thought microphone will be determined.

At first sight the problem seems very simple, at time t the imaginary moving microphone sees the sound pressure $p_m(t)$ which can be picked up from the pressure field $p(t,\mathbf{r}(t))$:

$$p_m(t) = p(t,x(t)). \tag{15}$$

Where $x(t)$ is the position of the imaginary microphone (see fig. 3). If we would be able to reconstruct the pressure as time series for each relevant position one could use samples t_i from eq. (15), apply an A-filter to the resulting time series, use (5) an the work is done. Unfortunately we got only a kind of STFFT which is not trivially convertible to a time series. Furthermore the SIFAH algorithm has relatively high computational costs, so that we can't calculate the extrapolation for all sampled positions. Therefore the problem is a little more sophisticated.

First we use SIFAH to determine the STFFT blocks on M positions x_j, equally distributed over the interval $[-15\text{m}, 15\text{m}]$, as it is sketched in fig. 3. For each position we get Q spectra which are treated as STFFT of the pressure signals. The position of the imaginary microphone can be calculated from the vehicles' velocity:

$$x(t) = -\int_{t_0}^{t} \mathrm{d}t'\, v_v(t'), \quad x(t_0) = -15m, \tag{16}$$

where t_0 is a trigger time, which marks the begin of the pass-by. Note that $y = 1.2$ m and $z = 7.5$ m are constants and therefore suppressed here.

Analogous to the estimation of the A-weighted sound pressure at a fixed position (7) we use

$$p_{m(A)}(t_i) = \sum_{k_{\min}}^{k_{\max}} A(k) \underbrace{\left(w_1 B_{i,k}(x_j) + w_2 B_{i,k}(x_{j+1})\right)}_{=B^m_{i,k}} \tag{17}$$

to estimate the A-weighted RMS-Fast value from the perspective of the imaginary microphone. The index j is chosen so that $x_j < x(t_i) \leq x_{j+1}$. We introduced the weighting factors

$$w_1 = \frac{|x_m(t_s) - x_{j+1}|}{|x_j - x_{j+1}|} \quad w_2 = \frac{|x_m(t_s) - x_j|}{|x_j - x_{j+1}|}, \tag{18}$$

which weight the contribution of the SIFAH on the neighbor positions according to the distance of the current position to the imaginary microphone. The $B^m_{i,k}$'s are coefficients of the series of spectra $\mathbf{B}^m_i$ which are treated as the STFFT of the imaginary moving microphone. The results of equation (17) were then used in (8) to get the SIFAH estimation for the A-weighted RMS-Fast output of the imaginary microphone. Together with the trajectory $x(t)$ we can compute a pass-by curve in parametric representation: $\left[x(t), L(p^2_{(A)m}(t))\right]$.

Note that the number of support points resulting from (17) is the same as the number of blocks Q used for the initial FFT in SIFAH. If one uses a small overlap to save computational time, the step function character of equation (8) becomes visible in the resulting curve. To address this issue as good as possible, instead of associating the energy in one block with one time point, we use the same block for a couple of time points within the the corresponding time interval. This means we use the blocks multiple times but with adapted weight functions or even other values of j corresponding to the movement of the imaginary microphone meanwhile. While the time resolution is not improved by that, at least a benefit from an increased spatial resolution will be achieved.

4 Measurements

4.1 Setup

All measurements were performed with a sampling rate of 48 kHz. The length of the FFT blocks was $N = 4096$ samples and a von Hann window was applied to each block before the transformation. The minimal overlap per block was set to 80 percent and the maximal degree

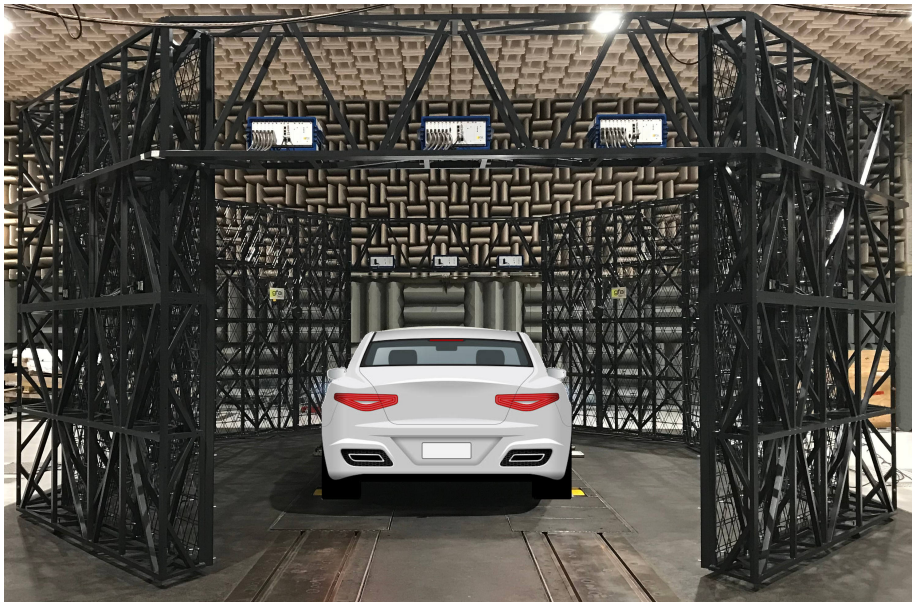

Figure 4: Arrangement of the microphone array in a test rig. The vehicle is enveloped by 864 microphones, 432 on each side. The vehicle shown is an artificially generated symbol image.

of the SIFAH algorithm was $l = 35$. The evaluated frequency interval covers 44.7 Hz to 3558.0 Hz if nothing else is mentioned.

Calibration

For the calibration of the algorithm parameters, nine microphones of type PCB 130c20 were placed on the right hand side in relation to the driving direction (see fig. 5). The measurements were carried out with a standard noise source (26 Measurements), and two vehicles (14 and 26 Measurements). The evaluation of the measured data showed that the SIFAH results were well suited for moderately high frequencies (approx. 2000 Hz), however for lower frequencies we saw only coincidence with the reference measurements when full reflections were taken into account. This transition is represented by (11). The measurements on the first vehicle together with the reference microphones were used to optimize the coefficient of reflection. We assumed a constant coefficient of reflection for each third octave between 44.7 Hz and 3548 Hz and calculated the resulting level curves using SIFAH as it is described in section 3.1. The level curves obtained from the measurements with microphones M1, M2, M3 and M4 (see fig. 5) were used as reference. The optimum was defined so that the sum of (14) over the four microphones becomes minimal. For this purpose a BFGS method [1] was used. We compared the assumption of coherent (9) and incoherent (10) reflections and found, that the incoherent summation leads to a better match. The optimization result is shown figure 6. From the resulting $\alpha(f)$ curve we estimated the parameters of the model (11). Note that we also tried to use models with more parameters to fit the data, e.g. with an additional plateau for intermediate frequencies, but saw no benefit compared to the simple model. Eventually we found $f_l = 270$ Hz and $f_u = 1793$ Hz. These parameters were determined once and then used

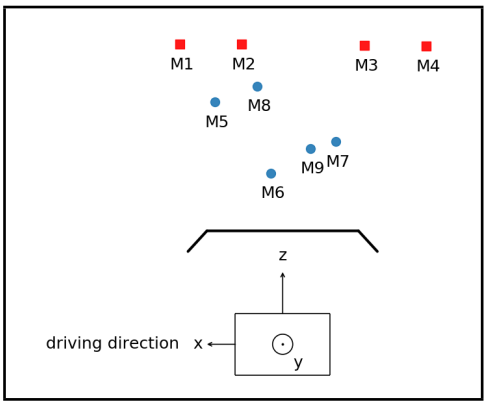

Microphone	x in m	y in m	z in m
M1	5.42	1.19	7.53
M2	2.16	1.20	7.52
M3	-4.33	1.19	7.49
M4	-7.58	1.21	7.48
M5	3.58	1.89	6.12
M6	0.62	1.59	4.40
M7	-2.82	0.80	5.16
M8	1.35	0.24	6.51
M9	1.48	0.24	5.0

Figure 5: Setup for calibration measurements: Nine microphones were placed behind the SIFAH array in order to record reference signals. The microphones marked as red squares were used to optimize the reflection coefficient. The table next to the picture shows the positions of the reference microphones. The origin of the coordinate system is at floor level.

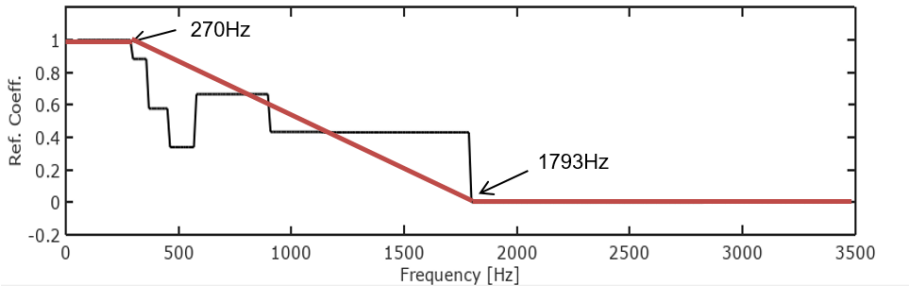

Figure 6: Reflection coefficients optimized per third octave: The black curve represents the result of the optimization, the red curve was finally used as model for the coefficient.

for all further measurements without further adaptations[3].

Verification

In the test rig, the PAK System of Müller-BBM is installed (see [11]). It is a well established system for simulated pass-by measurements. Seventeen microphones are placed on each side of the vehicle at a distance of 7.5 meters, covering a range from 8 meters in front of the vehicle to 8 meters behind the vehicle. Additionally measurement microphones of type PCB 130c20 were placed on the left front, left middle, right middle and right rear position of the PAK microphone arrangement (see Fig. 7).

All measurements were performed simultaneously with the microphone array, the PAK system and the PCB130c20 devices. Then the sound level on the marked positions in fig. 7 were

[3]Note that the parameter would change if the array would be transferred to an other environment.

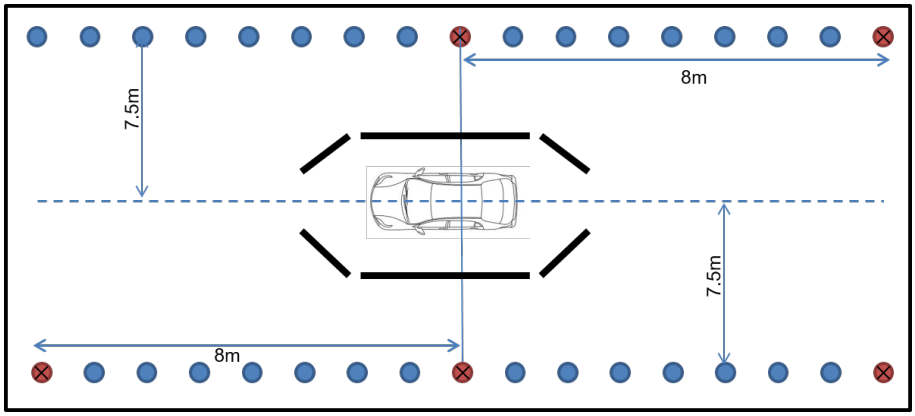

Figure 7: Sketch of the measurement setup. The sound source (e.g. a vehicle) is surrounded by the microphone array. In a distance of 7.5 meters left and right from the vehicle are lines of microphones from the PAK measurement system (circles) 1.2m over the ground. Additionally PCB 130c20 measurement microphones were placed nearly on the same position as four of the PAK microphones (red, crossed).

extrapolated using SIFAH and compared with the measured sound levels from the PAK and the PCB130c20 microphones. In order to verify the simulated pass-by noise levels the corresponding results from the PAK PASS-BY 2.0 software were used. Four different vehicles were measured on different days, denoted in the following with V1, V2, V3 and V4. The following measurements were performed for each of these vehicles: A pass-by with full throttle started at 50 km/h - 5 repetitions per vehicle and pass-by measurements with constant velocity of 30 km/h, 50 km/h and 70 km/h - for each 2 repetitions per vehicle. In total our verification is based on 44 measurement series.

4.2 Results

Figure 8 shows a comparison of the SIFAH sound level extrapolation with measured data at the marked positions in fig. 7. At each of these positions two microphones were placed close together. From the resulting time series, the A-weighted RMS/FAST was calculated according to (5), and compared to the level of the SIFAH output calculated according to (8). The deviations of the levels between the measurements from both microphones are of same order of magnitude as the deviations between SIFAH and the microphones. Therefore we state that the method works very well. Also the deviations according to (14) are always smaller then one decibel.

Additionally we verified the quality of the SIFAH approximation for all third octave bands between 44.7 Hz and 3548.0 Hz. Figure 9 shows some of the results. For frequencies smaller than approx. 120 Hz we see moderately good agreement, but for frequencies above the extrapolated data fits the measurement very well. At the upper edge of the frequency range used, the deviations begin to grow. This is in line with our expectations because the array is designed for a maximum frequency of around 3000 Hz for holography.

Figure 10 shows the pass-by channels calculated with SIFAH in comparison with the pass-by channels from the PAK system for V3 and V4. The curves for V1 and V2 look similar but are not shown here for due to lack of space.

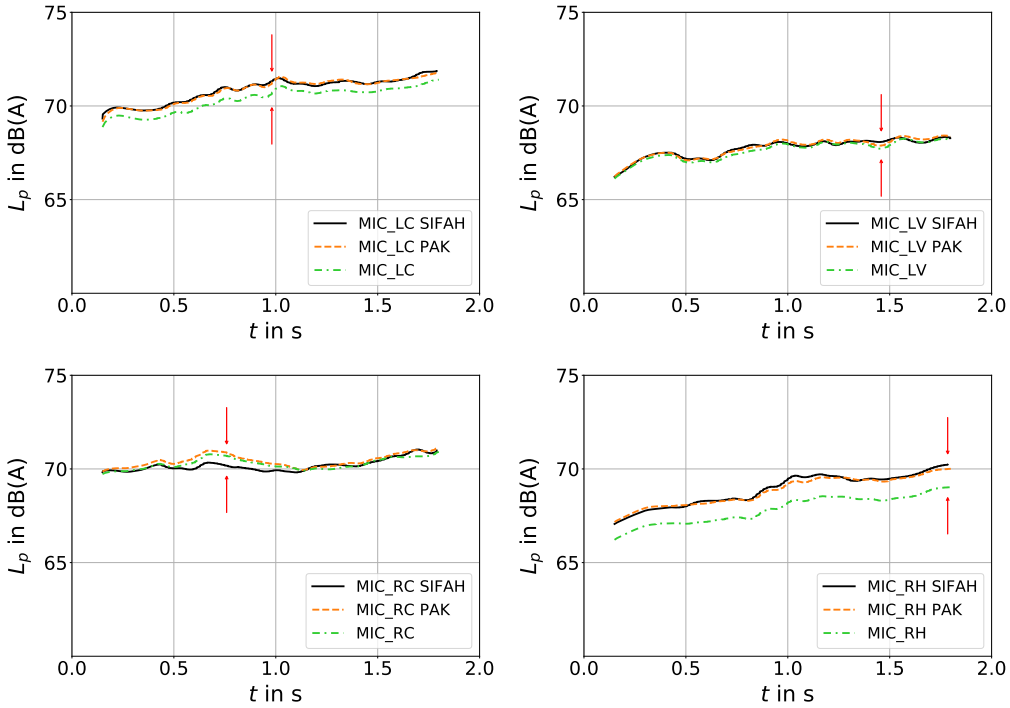

*Figure 8: Comparison of level profiles for V1. Level profiles for the PAK microphones (green), the PCB130c20 microphones (blue) and the result of the SIFAH algorithm (orange) on position left-front (*MIC_LV*), left-middle (*MIC_LC*), right middle (*MIC_RC*) and right rear (*MIC_RH*) are shown. The frequency interval considered ranged from* 44.7 *Hz* – 3548.0 *Hz. The arrows mark the sample with the maximal deviation.*

In order to quantify the deviations from the reference data, we considered the following quantities: The maximal level predicted by both systems, the position at which the maximum level is reached, the average deviation according to (14) and the maximal deviations according to eq. (13). Table 1 shows these quality markers for all measurements of accelerated pass-by. The values for the constant velocity pass-by measurements are of the same magnitude. The deviation of the maximal level is always less than one dB(A). Also our measure for the mean and the max deviation is, except one time, lesser than one decibel. The difference Δx between the positions where the maximal level is predicted by both systems lies between 0.1m and 6m. At first glance, this may appear to be large, but large values occur only in curves, where there is a range around the maximum within both curves are nearly constant. Little fluctuations, of magnitude some tenth dB(A), decide where on this interval the maximum lies. Therefore we are convinced that these deviations are not a problem.

5 Conclusion

We have demonstrated that the SIFAH method [9, 10] can be used for the extrapolation of sound level curves in intermediate distances from measurements close to the source of noise. An

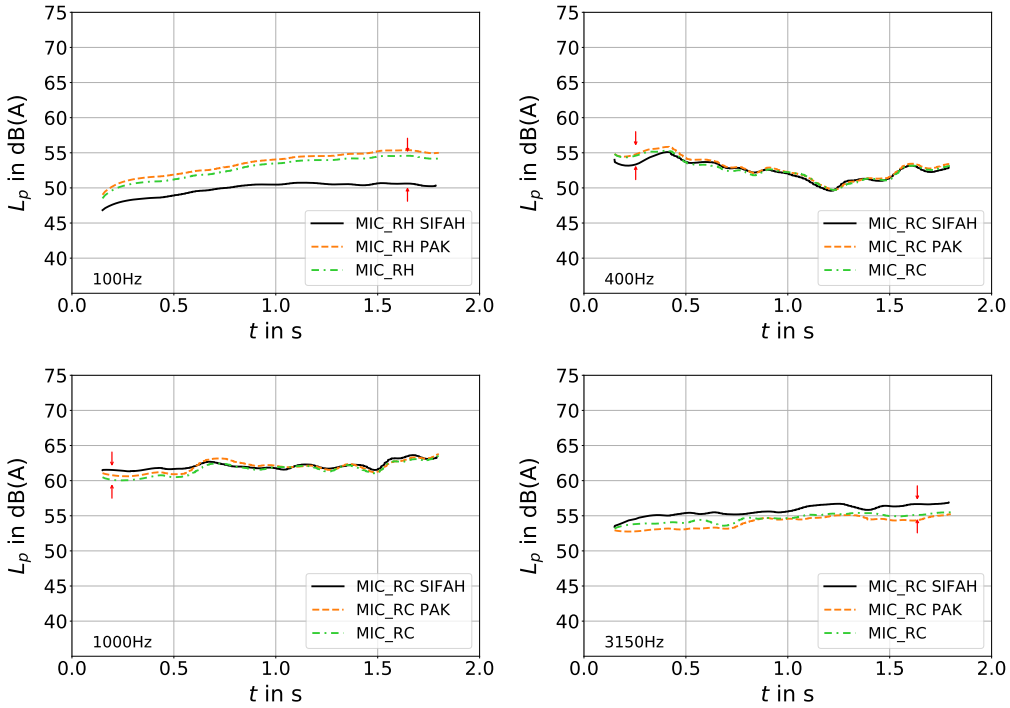

Figure 9: Comparison of measurements on V1 performed with two microphones to the SIFAH results for different frequency bands on position right center. The Level curves for the 100 *Hz,* 400 *Hz,* 1000 *Hz and* 3150 *Hz third octave bands are shown. The arrows mark the sample with the maximal deviation.*

array of 864 microphones was used for this purpose. It was designed to support both, classical beamforming and SIFAH, the latter up to frequencies of approx. 3000 Hz. In order to verify the SIFAH results reference measurements were made with microphones behind the array. The influence of reflections on the ground was investigated. We found good a agreement between the reference measurements and the SIFAH results. The deviations of the measurements from two microphones at almost the same location are of the same order of magnitude as the deviations of the SIFAH results from these microphones (approximately 1 dB(A)). The possibility to simulate noise emissions during a pass-by using SIFAH was shown. For this purpose some vehicles have been measured in a test rig. The results of an well established system for pass-by simulations (PAK) was used as reference. Both systems are predicting very similar curves, the deviations are almost always smaller than one dB(A).

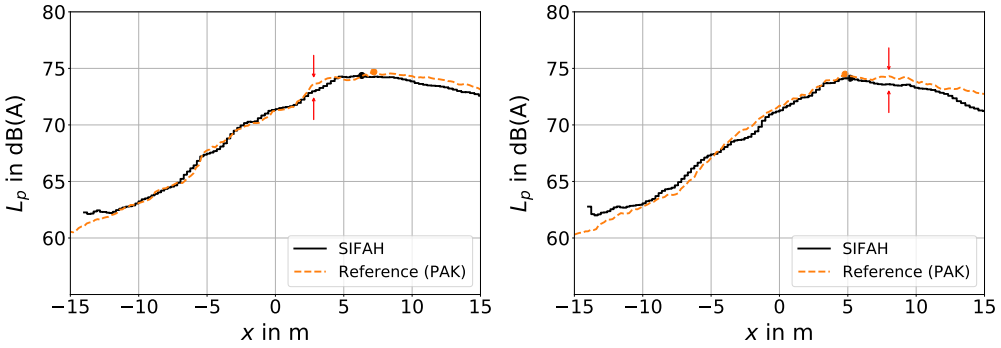

(a) Level curves for accelerated pass-by,Vehicle 3

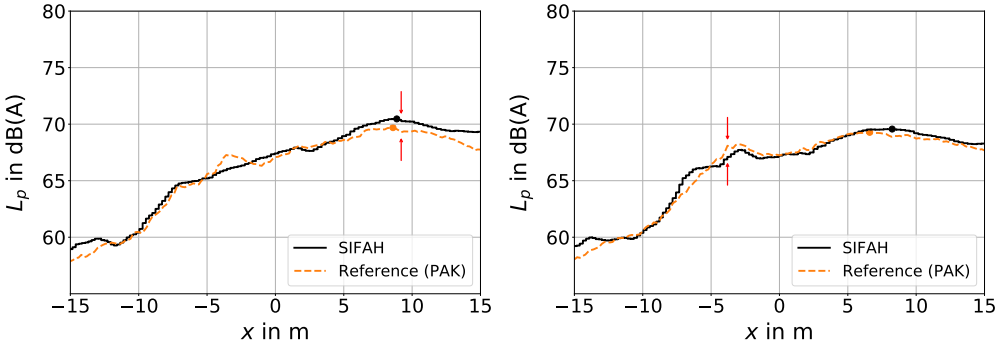

(b) Level curves for accelerated pass-by,Vehicle 4

Figure 10: Simulated pass-by level curves, generated from SIFAH extrapolation data, compared to simulated pass-by curves, generated by the well established PAK system. The curves in the left column show the pass-by for the left side of the car. The curves on the right column show the pass-by on the right respectively.

Table 1: Comparison of the maximal level of the virtual pass-by calculated with PAK: $L_{\max}$ and from SIFAH: $L_{\max}^{\mathrm{SIFAH}}$, difference of the position where that maximal level occurs and the deviation measures (13) *and* (14)*.*

	Left					Right				
	$L_{\max}^{\mathrm{PAK}}$ in dB(A)	$L_{\max}^{\mathrm{SIFAH}}$ in dB(A)	$\Delta x_{\max}$ in m	$\overline{\varepsilon}_{\max}$ in dB	$\overline{\varepsilon}$ in dB	$L_{\max}^{\mathrm{PAK}}$ in dB(A)	$L_{\max}^{\mathrm{SIFAH}}$ in dB(A)	$\Delta x_{\max}$ in m	$\overline{\varepsilon}_{\max}$ in dB	$\overline{\varepsilon}$ in dB
V 1	71.16	71.00	4.54	0.62	0.24	70.98	71.00	5.47	0.68	0.28
	71.58	71.34	0.22	0.61	0.22	70.60	70.73	3.10	0.24	0.60
	71.62	71.22	0.12	0.60	0.23	70.91	70.79	5.86	0.67	0.27
	71.86	70.84	0.19	0.63	0.21	70.66	70.52	5.34	0.58	0.20
	71.09	70.99	0.23	0.67	0.21	71.88	70.79	5.09	0.49	0.25
V 2	71.67	71.46	1.09	0.48	0.10	70.93	70.76	1.66	0.64	0.23
	71.64	71.26	0.07	0.46	0.13	70.60	70.42	0.00	0.76	0.30
	71.68	71.53	1.38	0.44	0.12	70.98	70.96	0.56	0.74	0.24
	71.55	71.19	0.36	0.35	0.12	70.97	70.51	0.16	0.69	0.30
	71.90	71.67	0.72	0.35	0.11	71.19	71.14	0.13	0.51	0.20
V 3	74.45	74.14	2.49	0.83	0.18	75.26	74.33	0.77	0.87	0.29
	74.70	74.49	0.59	0.51	0.11	74.49	74.23	0.09	0.48	0.17
	75.36	75.05	1.57	0.70	0.15	75.45	75.47	0.06	0.57	0.16
	75.47	75.11	0.31	0.50	0.13	74.81	74.82	0.09	0.41	0.12
	75.11	74.96	0.65	0.14	0.35	75.08	74.88	1.67	0.49	0.16
V 4	69.50	70.25	0.64	0.84	0.26	69.22	70.00	0.19	0.97	0.27
	69.56	70.32	1.91	0.94	0.29	69.12	69.68	0.42	0.66	0.18
	69.69	70.46	0.28	1.01	0.29	69.28	69.57	1.65	0.62	0.24
	68.99	69.76	0.35	0.83	0.23	68.67	69.01	0.52	0.67	0.23
	69.33	69.65	1.20	0.61	0.22	69.06	69.19	0.28	0.35	0.12

6 Acknowledgments

The authors gratefully acknowledge Dr. Olaf Jaeckel for stimulating discussions and proofreading of the manuscript.

REFERENCES

[1] R. Fletcher. *Practical methods of optimization*. John Wiley & Sons, New York, 1987. ISBN 978-0-471-91547-8.

[2] D. W. Griffin and J. S. Lim. "Signal estimation from modified short-time fourier transform." *IEEE Transactions on Acoustics, Speech, and Signal Processing*, 32(2), 236 – 243, 1984. ISSN 0096-3518.

[3] S. I. Hayek. *Nearfield Acoustical Holography*, pages 1129–1139. Springer New York, New York, NY, 2008. ISBN 978-0-387-30441-0. doi:10.1007/978-0-387-30441-0_59. URL https://doi.org/10.1007/978-0-387-30441-0_59.

[4] L. Landau and E. Liftschitz. *Lehrbuch der Theoretischen Physik, Band IV Hydrodynamik*. Verlag Europa Lehrmittel, 1991. ISBN 978-3-8085-5554-5.

[5] Y. Masuyama, K. Yatabe, Y. Koizumi, Y. Oikawa, and N. Harada. "Deep griffin–lim iteration." In *44th International Conference on Acoustics, Speech, and Signal Processing (ICASSP 2019)*. IEEE, 2019.

[6] M. A. Mironov and V. V. Pislyakov. "One-dimensional acoustic waves in retarding structures with propagation velocity tending to zero." *Acoustical Physics*, 48(3), 347–352, 2002. doi:10.1134/1.1478121.

[7] M. Möser. *Messtechnik der Akustik*. Springer Berlin Heidelberg, 2010.

[8] N. Perraudin, P. Balazs, and P. L. Sondergaard. "A fast griffin-lim algorithm." In *2013 IEEE Workshop on Applications of Signal Processing to Audio and Acoustics*. IEEE, 2013. doi:10.1109/waspaa.2013.6701851.

[9] C. Puhle. "Spherical integration in acoustical holography." In *48th International Congress and Exposition on Noise Control Engineering, 16-19 June, Madrid, Spain*. 2019.

[10] C. Puhle. "Spherical acoustical holography using planar microphone arrays." In *Proceedings of the 8th Berlin Beamforming Conference, 2 - 3 March 2020*. GFaI, Gesellschaft zu Förderung angewandter Informatik e.V., Berlin, 2020.

[11] Y. Ryu. "The optimum array design for the indoor simulated pass-by noise measurement system." In *Sound and Vibration International Congress*. 2005.

[12] A. Sommerfeld. *Partial Differential Equations in Physics*. Academic Press, New York, 1949.

[13] S. F. Wu. *The Helmholtz Equation Least Square Methods*. Springer, 2015.